Quasi-two-dimensional extraordinary Hall effect

N. Ryzhanova,[1,2] A. Vedyayev,[1,2] A. Pertsova,[3] and B. Dieny[1]
[1]*SPINTEC, CEA/CNRS, URA 2512, 38054 Grenoble Cedex 9, France*
[2]*Department of Physics, M.V. Lomonosov Moscow State University, Leninskie Gory, 1199991 Moscow, Russia*
[3]*School of Physics and CRANN, Trinity College Dublin, Dublin 2, Ireland*
(Received 27 December 2008; revised manuscript received 8 June 2009; published 10 July 2009)

Quasi-two-dimensional transport is investigated in a system consisting of a very thin ($\approx$1 nm) ferromagnetic layer sandwiched between two insulating layers. Using the mechanism of skew scattering to describe the extraordinary Hall effect (EHE) and calculating the conductivity tensor, we compare the quasi-two-dimensional Hall resistance with the Hall resistance of a massive sample. In this study, a mechanism of EHE (geometric mechanism of EHE) due to nonideal interfaces and volume defects is also proposed.

DOI: 10.1103/PhysRevB.80.024410 PACS number(s): 75.47.−m, 75.70.−i, 73.50.Jt

I. INTRODUCTION

Recently there has been an increased interest in the design and fabrication of new spintronic devices based on the tunnel magnetoresistance effect[1] and the recently discovered spin torque effect[2] in multilayered structures consisting of several ferromagnetic nanolayers separated by thin insulating barriers. The geometry of such structures also provides the possibility to investigate some of their quasi-two-dimensional transport properties and particularly to compare the relationship between diagonal and off-diagonal [responsible for extraordinary Hall effect (EHE)] conductivities in massive and above-mentioned samples. This study is of great interest to the field of spintronics since quasi-two-dimensional EHE may provide an additional mechanism for storing and processing information in logic devices.

Basically, three mechanisms of EHE are considered in the literature. The first mechanism is the skew scattering, introduced by Smit[3] and investigated in details in Ref. 4. The second one is the side-jump mechanism introduced by Berger.[5] Both of these mechanisms are extrinsic, as it was clarified in Refs. 6 and 7; however, the third mechanism is intrinsic. It was first discovered by Karplus and Luttinger[7] and has been recently reinvestigated in a number of works[8,9] using the concept of the Berry's phase.

In this paper, we studied the influence of the size effect on EHE in a thin ferromagnetic film sandwiched between two insulating barriers. In general, the size effect in any transport properties of thin films can be experimentally observed in the case when the thickness of the film is smaller than the elastic mean-free path or, in other words, when the concentration of impurities in the bulk of the sample is small. We have to mention here that the side-jump mechanism gives contributions to EHE proportional to ρ^2, where ρ is the resistivity of the sample, while the skew scattering contribution to EHE is proportional to ρ. Therefore, for clean samples, where the size effect may be experimentally observed, the skew scattering is the dominant mechanism of EHE. Besides that, the intrinsic contribution to EHE due to the Berry curvature depends on the details of the electronic structure, which is less sensitive to the interface scattering than the usual size effect. In recent theoretical works,[10–13] all three contributions to EHE were studied in detail. In Refs. 10–12, a two-dimensional ferromagnet with Rashba spin-orbit interaction was considered and in Ref. 13 a more general solution including three-dimensional samples was investigated. An interesting result was obtained in Ref. 12, where it was proven that three approaches to the problem, namely, Keldysh, Boltzmann, and Kubo formalisms, give the same results for EHE. For us it is important to point out that in Refs. 10–13 it was shown that the skew scattering is the dominant mechanism of EHE for small concentration of impurities, e.g., for large mean-free paths of electrons, which is the situation treated in the present paper. We also note that in the literature cited above, the size effect was not taken into account. We can mention the work of Ryzhanova *et al.*,[14] where the influence of the size effect on EHE was investigated in the system consisting of two ferromagnetic layers with antiparallel magnetizations and a paramagnetic metallic spacer. In that work, the size effect was due to the difference between the mean-free paths of electrons with "up" and "down" projections of the spin but additional scattering of electrons at the interfaces was not considered.

The present paper is organized as follows. In Sec. II, we present the model of EHE based on the mechanism of skew scattering on the bulk and interfacial impurities. We report our results for the conductivity tensor including finite-size terms calculated within the framework of Kubo formalism. We also compare the quasi-two-dimensional Hall resistance (ρ^H_{2D}) with that of a massive sample (ρ^H_{bulk}). Section III discusses the nonideality of the interfaces and the existence of volume defects that affect the form of current lines. We propose a mechanism of EHE (we will refer to it as the geometric mechanism of EHE) due to these defects using the diffusion equation[15] and taking into account that the diffusion coefficient has an off-diagonal component proportional to the spin-orbit interaction. We summarize our results and draw some conclusions in Sec. IV. The details of some calculations are shown in the Appendix.

II. SKEW-SCATTERING MECHANISM OF EHE IN A THREE-LAYERED STRUCTURE

We consider a system consisting of a ferromagnetic metallic layer (F) sandwiched between two insulating layers (I). The magnetization of the ferromagnetic layer is along the z

direction, perpendicular to the interfaces. The first interface (I/F) is considered to be ideally reflecting while the second one (F/I) is considered as rough so that electrons crossing this interface undergo diffusive spin-dependent scattering.

The electric current is parallel to the y axis resulting in the appearance of the Hall field along x direction. In this case

$$\begin{pmatrix} j_x \\ j_y \end{pmatrix} = \begin{pmatrix} 0 \\ j_y \end{pmatrix} = \begin{pmatrix} \sigma_{xx} & \sigma_{xy} \\ \sigma_{yx} & \sigma_{yy} \end{pmatrix} \begin{pmatrix} E_x^H \\ E_y \end{pmatrix},$$

$$E_x^H = -\frac{\sigma_{xy}}{\sigma_{xx}} E_y,$$

$$\rho_{2D,bulk}^H = \frac{\sigma_{yx}}{\sigma_{yy}\sigma_{xx} + \sigma_{yx}^2}, \tag{1}$$

where j_α are the current-density components, $\sigma_{\alpha\beta}$ are diagonal and off-diagonal conductivities, E_x^H is the Hall field, and E_y is the y component of the electric field.

The Hamiltonian $\hat{H}$ of the system can be written as

$$\hat{H} = \frac{\hat{p}^2}{2m} + \sum_n U(r - R_n) + \sum_n H_{so}(r - R_n), \tag{2}$$

where $U(r-R_n)$ is the potential of impurities, and H_{so} is the spin-orbit interaction between the orbit of electron and the spin of the impurity. The matrix element of $H_{so}(r-R_n)$ is given by Eq. (5).

For the calculation of $\rho_{2D,bulk}^H$, we use the Kubo formula with vertex corrections responsible for the transverse component of the current

$$\sigma_{\alpha\beta} = \frac{\hbar e^2}{\pi a_0^4} \sum_{\kappa\kappa' z'} G_{\kappa\kappa'}^+(zz') \nu_{\kappa\alpha} G_{\kappa'\kappa}^-(z'z) \nu_{\kappa'\beta}, \tag{3}$$

where $\vec{\nu_\kappa}$ is the velocity vector along the interface, $G_{\kappa\kappa'}^+(zz')$ and $G_{\kappa'\kappa}^-(zz')$ are, respectively, advanced and retarded Green's functions in mixed coordinate-momentum representation, and a_0 is the lattice constant. To calculate the y-x component of the conductivity tensor, we use the perturbation theory and take into account only the corrections in linear order of the spin-orbit interaction

$$G_{\kappa\kappa'}^+(zz') = G_{0\kappa}^+(zz')\delta_{\kappa\kappa'} + G_{0\kappa}^+(zz'')\sum_{\vec{\rho}} [T_{\kappa\kappa'}^+(\vec{\rho}z'') + H_{\kappa\kappa'}^{so}(\vec{\rho}z'')] G_{0\kappa'}^+(z''z'), \tag{4}$$

$$H_{\kappa\kappa'}^{so}(\vec{\rho}z'') = i\lambda^{so}(\vec{\rho}z'') a_0^2 m_z [\kappa\kappa']_z, \tag{5}$$

where $T_{\kappa\kappa'}^+(\vec{\rho}z)$ and $H_{\kappa\kappa'}^{so}(\vec{\rho}z)$ are, respectively, the scattering matrix and the spin-orbit interaction, dependent on the type of atom at $(\vec{\rho}z)$ position; $\vec{m_z}$ is the unit vector along the magnetization and λ^{so} is the spin-orbit parameter. Taking into account that $[\kappa \times \kappa']_z = \kappa_x\kappa_y' - \kappa_x'\kappa_y$, it follows from Eq. (5) that $H_{\kappa\kappa'}^{so}(\vec{\rho}z'') = -H_{\kappa'\kappa}^{so}(\vec{\rho}z'')$.

The T matrix in one-site approximation is written as

$$T_{\kappa\kappa'}(\vec{\rho}z) = \sum_n \frac{[\epsilon_n - \Sigma(z)] e^{i(\kappa-\kappa')(\vec{\rho}-\vec{\rho_n})}}{1 - [\epsilon_n - \Sigma(z)] G(\vec{\rho_n}z, \vec{\rho_n}z)}, \tag{6}$$

$$\lambda_{\kappa\kappa'}^{so}(\vec{\rho}z) = \sum_m e^{i(\kappa-\kappa')(\vec{\rho}-\vec{\rho_m})} \lambda_m^{so}, \tag{7}$$

where ϵ_n is the one-site energy and

$$G(\vec{\rho_n}z, \vec{\rho_n}z) = \frac{a_0^2}{\pi} \int_0^{\sqrt{2\pi}/a_0} \kappa G_\kappa(zz) d\kappa.$$

For the binary system AB, ϵ_n and λ_m^{so} take values $\epsilon_{A,B}$ and $\lambda_{A,B}^{so}$, respectively. In Eq. (6) $\Sigma(z)$ is the coherent potential that can be found from the system of self-consistent equations. The first equation of the system is valid for scattering on both bulk and interfacial impurities,

$$\frac{[\epsilon_A - \Sigma(z)] c_A}{1 - [\epsilon_A - \Sigma(z)] G_0(\vec{\rho_n}z, \vec{\rho_n}z)} + \frac{[\epsilon_B - \Sigma(z)] c_B}{1 - [\epsilon_B - \Sigma(z)] G_0(\vec{\rho_n}z, \vec{\rho_n}z)} = 0, \tag{8}$$

while the second one is written in the form corresponding only to the interfacial scattering since we are interested in calculating the interfacial coherent potential

$$G(\vec{\rho_n}z, \vec{\rho_n}z) = \frac{G_0(\vec{\rho_n}z, \vec{\rho_n}z)}{1 - \Sigma(z) G_0(\vec{\rho_n}z, \vec{\rho_n}z)}. \tag{9}$$

For the calculation of σ_{xx} and σ_{yy}, we use Eq. (3) with Green's functions diagonal on κ and renormalized on the coherent potential. For the off-diagonal component of the conductivity, averaging over the impurity distribution yields

$$\sigma_{yx} = \frac{\hbar^3 e^2 m_z}{\pi a_0^2 m^2} \sum_{\kappa\kappa' \vec{\rho_n}} \kappa_y^2 \kappa_x'^2 |G_\kappa^+(zz'')|^2 |G_\kappa^+(z'z'')|^2 \times \mathrm{Im}[T_{\kappa\kappa'}^+(\vec{\rho_n}z'') \lambda_{\kappa'\kappa}^{so}(\vec{\rho_n}z'')], \tag{10}$$

where $(\vec{\rho_n}z'')$ is the impurity position. We keep in Eq. (10) only the main term with $n=m$.

For the binary AB structure and purely random distribution of A and B, summing over $\vec{\rho_n}$ gives $\delta_{\kappa\kappa'}$. It is convenient to divide λ^{so} into average and scattering parts

$$\lambda_A^{so} = c_A\lambda_A^{so} + c_B\lambda_B^{so} + c_B\lambda_A^{so} - c_B\lambda_B^{so} = \bar{\lambda} + c_B\delta\lambda^{so}, \tag{11}$$

$$\lambda_B^{so} = c_A\lambda_B^{so} + c_B\lambda_B^{so} + c_A\lambda_A^{so} - c_A\lambda_A^{so} = \bar{\lambda} - c_A\delta\lambda^{so}. \tag{12}$$

The average in Eq. (10) is

$$\frac{1}{N}\sum_n \langle T_n(z)\lambda_n^{so}(z)\rangle \approx \bar{\lambda}(c_A\Phi_A + c_B\Phi_B) + \delta\lambda^{so} c_A c_B (\Phi_A - \Phi_B), \tag{13}$$

Where

$$\Phi_A = \frac{[\epsilon_A - \Sigma(z)]}{1 - [\epsilon_A - \Sigma(z)] G(\vec{\rho_n}z, \vec{\rho_n}z)}, \tag{14}$$

$$\Phi_B = \frac{[\epsilon_A - \Sigma(z)]}{1 - [\epsilon_A - \Sigma(z)] G(\vec{\rho_n}z, \vec{\rho_n}z)}. \tag{15}$$

According to Eq. (8), we only take the imaginary part of the last term in Eq. (13). We then rewrite Eq. (13) with renormalized Green's function

$$\mathrm{Im}\left[\frac{1}{N}\sum_n \langle T_n(z)\lambda_n^{so}(z)\rangle\right] \approx \delta\lambda^{so}c_A c_B \times \mathrm{Im}\left\{\frac{[\epsilon_A-\Sigma(z)][1-\Sigma(z)G_0(\vec{\rho_n}z,\vec{\rho_n}z)]}{1-\epsilon_A G_0(\vec{\rho_n}z,\vec{\rho_n}z)} - \frac{[\epsilon_B-\Sigma(z)][1-\Sigma(z)G_0(\vec{\rho_n}z,\vec{\rho_n}z)]}{1-\epsilon_B G_0(\vec{\rho_n}z,\vec{\rho_n}z)}\right\}, \tag{16}$$

$$G_0(\vec{\rho_n}z,\vec{\rho_n}z) \equiv F_0(z). \tag{17}$$

Equation (8) for coherent potential is

$$\Sigma(E,z) = \bar{\epsilon} + \frac{c_A c_B \delta^2 F(E,z)}{1-[\tilde{\epsilon}-\Sigma(E,z)]F(E,z)}, \tag{18}$$

where $\bar{\epsilon}=c_A\epsilon_A+c_B\epsilon_B$, $\tilde{\epsilon}=c_A\epsilon_B+c_B\epsilon_A$, and $\delta=\epsilon_A-\epsilon_B$.

Usually it is convenient to choose $\bar{\epsilon}=0$. In this case $\tilde{\epsilon}=-(c_A-c_B)\delta$, $\epsilon_A=c_B\delta$, and $\epsilon_B=-c_A\delta$.

Next we assume that the scattering parameters for bulk impurities such as the scattering potential and concentration are small enough to keep only the main terms for all values. In this case, the imaginary part of Σ is on the order of δ^2 so that, for σ_{yx}^{bulk}, it remains

$$\mathrm{Im}\left(\frac{1}{N}\sum_n \langle T_n(z)\lambda_n^{so}(z)\rangle\right) \approx \delta\lambda_{bulk}^{so}\delta_{bulk}^2 c_A^{bulk}c_B^{bulk}(c_A^{bulk}-c_B^{bulk}) \times \mathrm{Im}\frac{F}{(1-c_B^{bulk}\delta_{bulk}\,\mathrm{Re}\,F)^2(1+c_A^{bulk}\delta_{bulk}\,\mathrm{Re}\,F)^2}. \tag{19}$$

For the interfacial values, the full self-consistent scheme is necessary. For both bulk and interfaces, we suppose that the real part of the coherent potential just represents the renormalization of electron spectrum so that Σ can be considered as purely imaginary.

The zero-order Green's function can be found from the Schrodinger equation in κ-z representation (we will further use the units with energy dimension $[L]=\dot{A}$)

$$G_{0\kappa}^{+}(0<z'<z<z_1) \approx \frac{1}{2ik_1((q+ik_1)^2e^{ik_1a}-(q-ik_1)^2e^{-ik_1a})}[(q-ik_1)e^{ik_1(z-z_1)}-(q+ik_1)e^{-ik_1(z-z_1)}][(q+ik_1)e^{ik_1z'}-(q-ik_1)e^{-ik_1z'}], \tag{20}$$

where

$$k_1=\sqrt{k_F^{\uparrow 2}-\kappa^2+i\frac{2k_F^{\uparrow}}{l_1}} \equiv c_1+id_1,$$

$$c_1=\sqrt{\frac{1}{2}\left[\sqrt{(k_F^{\uparrow 2}-\kappa^2)^2+\frac{4k_F^{\uparrow}}{l_1}}+(k_F^{\uparrow 2}-\kappa^2)\right]},$$

$$d_1=\sqrt{\frac{1}{2}\left[\sqrt{(k_F^{\uparrow 2}-\kappa^2)^2+\frac{4k_F^{\uparrow}}{l_1}}-(k_F^{\uparrow 2}-\kappa^2)\right]},$$

$$q=\sqrt{q_0^2+\kappa^2}\ q_0^2=\tfrac{2m}{\hbar^2}(U-E_F),$$

0 and z_1 are the coordinates of the left and right interfaces, a is the layer thickness; $k_F^{\uparrow}$ and l_1 are the Fermi momentum and the mean-free path for spin up, respectively, $c_1d_1=\kappa_F^{\uparrow}/l_1$ (for spin down we use indices $\downarrow$ and 2), U is the height of the potential barrier, and E_F is the Fermi energy. The poles of the Green's function in Eq. (20) define the quantized energy spectrum of the thin ferromagnetic layer.

A. Calculation of the bulk quasi-two-dimensional diagonal conductivity

For $\sigma_{xx}=\sigma_{yy}$ in Eq. (3), we take into account the scattering at the interface, which is responsible for the size effect, as well as the scattering in the bulk of the sample by using the Dyson equation with renormalized Green's function

$$G_\kappa(zz') = G_{0\kappa}(zz') + G_{0\kappa}(z0)\Sigma G_\kappa(0z') = G_{0\kappa}(zz') + \frac{G_{0\kappa}(z0)\Sigma G_{0\kappa}(0z')}{1-G_{0\kappa}(00)\Sigma}. \tag{21}$$

Integrating over z' from zero to z for $z'<z$ and from z to a for $z'>z$ gives the conductivity in the units Ω^{-1} cm^{-1}. The complete expression for the diagonal conductivity is shown in the Appendix. For sufficiently thick layers, averaging out the oscillations yields the averaged expression

$$\langle\sigma_{xx}^{\uparrow}\rangle = \frac{\sigma_0 l_1 10^8}{2\pi k_F^{\uparrow}}\int \frac{\kappa^3 d\kappa}{c_1}\left[1-\frac{l_1}{a}\frac{|\mathrm{Im}\,\Sigma|c_1\sinh 2d_1a}{(q^2+c_1^2+|\Sigma|^2+2q\,\mathrm{Re}\,\Sigma)\sinh 2d_1a+2c_1|\mathrm{Im}\,\Sigma|\cosh 2d_1a}\right], \tag{22}$$

where $\sigma_0=\frac{e^2}{2\pi\hbar}=\frac{10^{-3}}{13.6}(\Omega^{-1})$ is the elementary conductivity of one channel.

The first term in Eq. (22) is the conductivity of the massive sample whereas the second one is due to the quasiclassical finite-size effect. For the large thickness of the ferromagnetic layer ($a/l_1 \gg 1$), the latter term is small. However, in the opposite limit ($a/l_1 \ll 1$) the scattering at the interface becomes dominant and the total conductivity is proportional not to the bulk mean-free path but to the interfacial mean-free path, which is inversely proportional to Im Σ. The total

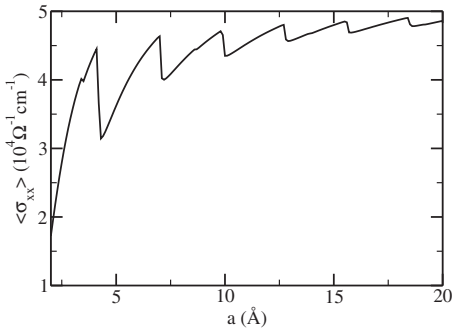

FIG. 1. Averaged diagonal conductivity as a function of the layer thickness a for $k_F^{\uparrow}=1.1(\dot{A}^{-1})$, $k_F^{\downarrow}=0.6(\dot{A}^{-1})$, $l_1=100(\dot{A})$, $l_2=60(\dot{A})$, and $c=0.3$.

conductivity given by the sum of the contributions from the two spin channels is shown in Fig. 1 as a function of the layer thickness.

B. Calculation of the off-diagonal conductivity due to the spin-orbit interfacial scattering

We now calculate $\sigma_{xy}^{\uparrow}(z)$ using Eq. (10) with the Green's function defined by Eq. (21) and $z''=0$ (see the Appendix). The averaged expression is given by

$$\langle\sigma_{xy}^{\uparrow}\rangle = \frac{\sigma_0 l_1 a_0^4 10^8}{8\pi^2 k_F^{\uparrow}} \int \kappa^3 d\kappa c_1 \frac{\mathrm{Im}\langle T(\vec{\rho}_n 0)\lambda^{so}(\vec{\rho}_n 0)\rangle \sinh 2d_1 a}{Den_3^{\uparrow}} \times \int \kappa^3 d\kappa \frac{\cosh 2d_1(z-a)}{Den_3^{\uparrow}}, \tag{23}$$

where

$$Den_3^{\uparrow} = (q^2 + c_1^2 + |\Sigma^-|^2 + 2q\ \mathrm{Re}\ \Sigma^-)\sinh 2d_1 a + 2c_1\ \mathrm{Im}\ \Sigma^- \cosh 2d_1 a. \tag{24}$$

The same calculation was carried out for spin down and the total off-diagonal conductivity is shown in Fig. 2.

Equation (23) describes the contribution to the Hall conductivity due to the additional spin-orbit scattering at the interface. Contrary to the usual conductivity that decreases with the thickness, this term increases because the additional skew scattering at the interface is more pronounced for small thicknesses.

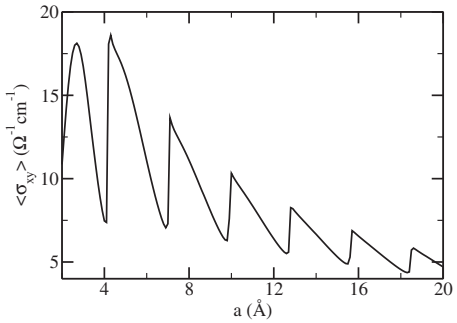

FIG. 2. Averaged off-diagonal conductivity as a function of the layer thickness a for $k_F^{\uparrow}=1.1(\dot{A}^{-1})$, $k_F^{\downarrow}=0.6(\dot{A}^{-1})$, $l_1=100(\dot{A})$, $l_2=60(\dot{A})$, $c=0.3$, and $\lambda^{so}=0.05(\dot{A}^{-1})$.

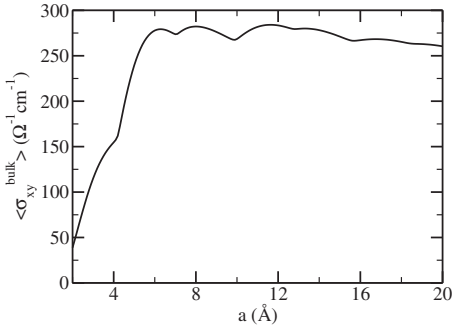

FIG. 3. Averaged bulk off-diagonal conductivity as a function of the layer thickness a for $k_F^{\uparrow}=1.1(\dot{A}^{-1})$, $k_F^{\downarrow}=0.6(\dot{A}^{-1})$, $l_1=100(\dot{A})$, $l_2=60(\dot{A})$, $\lambda_{bulk}^{so}=0.03(\dot{A})$, $c^{bulk}=0.01$, and $\delta_{bulk}=1(\dot{A}^{-1})$.

We also calculate the bulk off-diagonal conductivity $\sigma_{xy}^{\uparrow bulk}+\sigma_{xy}^{\downarrow bulk}$ (see Fig. 3) using Eq. (10) with additional integration over z''. For this calculation we use the bulk scattering parameters and the bulk coherent potential in Born approximation $\Sigma^{bulk}=ic^{bulk}(1-c^{bulk})\delta_{bulk}^2\,\mathrm{Im}\,F^{bulk}(zz)$. The details of the calculation can be found in the Appendix while the averaged expression is given below

$$\langle\sigma_{xy}^{\uparrow bulk}\rangle = \frac{\sigma_0 l_1^2 a_0^3\ \mathrm{Im}\langle T^{bulk}\lambda_{bulk}^{so}\rangle 10^8}{8\pi^2 k_F^{\uparrow 2}} \left\{\int \frac{\kappa^3 d\kappa}{c_1}\right\}^2. \tag{25}$$

In the case of a thin layer, $\langle\sigma_{xy}^{\uparrow bulk}\rangle$ shows an oscillating behavior but it tends to a constant value when $a\to\infty$, which coincides with its value for the massive sample. If we take into account the interfacial scattering, the expression for σ_{xy}^{bulk} becomes too complex so we do not show it here. But the thickness dependencies of σ_{xy}^{bulk} and the Hall angle $\rho^H/\rho\approx\sigma_{xy}/\sigma_{xx}$ (for $\sigma_{xy}\ll\sigma_{xx}$) calculated using the complete formula with renormalized Green's functions are presented in Figs. 4 and 5, respectively.

Besides that, it is interesting to check the validity of the phenomenological relationship between the Hall resistance ρ^H and $\rho=1/\sigma_{xx}$

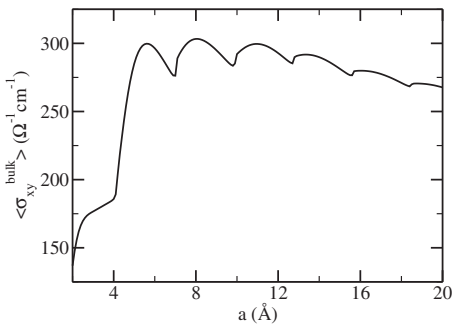

FIG. 4. Averaged bulk off-diagonal conductivity *with interfacial scattering* as a function of the layer thickness a for $k_F^{\uparrow}=1.1(\dot{A}^{-1})$, $k_F^{\downarrow}=0.6(\dot{A}^{-1})$, $l_1=100(\dot{A})$, and $l_2=60(\dot{A})$; bulk parameters $\lambda_{bulk}^{so}=0.03(\dot{A}^{-1})$, $c^{bulk}=0.01$, and $\delta_{bulk}=1(\dot{A}^{-1})$; interface parameters $\lambda^{so}=0.05(\dot{A}^{-1})$, $c=0.3$, and $\delta=1.5(\dot{A}^{-1})$.

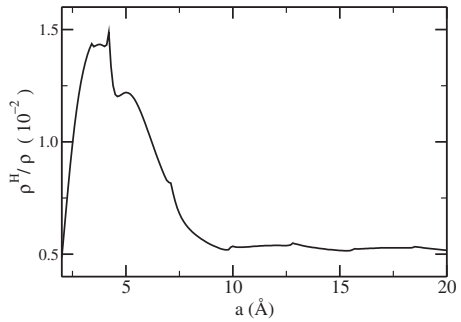

FIG. 5. Hall angle ρ^H/ρ as a function of layer thickness a for $k_F^{\uparrow}=1.1(\dot{A}^{-1})$, $k_F^{\downarrow}=0.6(\dot{A}^{-1})$, $l_1=100(\dot{A})$, and $l_2=60(\dot{A})$; bulk parameters $\lambda_{bulk}^{so}=0.03(\dot{A}^{-1})$, $c^{bulk}=0.01$, and $\delta_{bulk}=1(\dot{A}^{-1})$; interface parameters $\lambda^{so}=0.05(\dot{A}^{-1})$, $c=0.3$, and $\delta=1.5(\dot{A}^{-1})$.

$$\rho^H = b_1\rho + b_2\rho^2. \tag{26}$$

In order to do this, we plotted $\rho^H/\rho(\rho)$ in Fig. 6. As one can see, this curve may be divided into two regions where the dependence is approximately linear with different sign for the coefficient b_2; it is positive in quasiclassical limit of the size effect (large thickness a) and negative in ultraquantum region. We may explain this behavior as follows. In quasiclassical regime, the diagonal conductivity smoothly (if weak oscillations are neglected) decreases with increasing thickness, which is due to additional contribution of the interfacial electron scattering to the resistivity. On the contrary, the contribution to the Hall conductivity due to more intensive skew scattering at the interface increases so that the ratio σ_{xy}/σ_{xx} increases with increasing resistance. In ultraquantum regime, the diagonal conductivity continues to decrease due to a decrease in the number of conductivity channels while the skew scattering, responsible for the Hall conductivity, decreases more rapidly due to an additional decrease in the available phase space for scattering. As a result, the ratio σ_{xy}/σ_{xx} decreases with increasing resistance.

III. GEOMETRIC MECHANISM OF EHE

In the previous sections we considered the thin ferromagnetic film sandwiched between two insulating layers and took into account the additional scattering on the defects of the interfaces. However, in the case when the thickness of the ferromagnetic layer is small, it can become discontinuous due to the tendency of the metallic layer to coalesce when deposited on an oxide layer, i.e., some oxidized insulating columns can form inside the layer. We investigate the influence of this phenomenon on EHE. The insulating columns were modeled by insulating cylinders of radius R extending over the thickness of the metallic layer. The calculation was done using the approximation of diffusive transport. We note that in this section we do not give in detail the mechanism of EHE, assuming that we know the value of σ^{xy} for the sample without the insulating columns.

In the absence of precession, the diffusion equations are given by

$$\frac{\partial n}{\partial t} + \frac{\partial j_e^x}{\partial x} + \frac{\partial j_e^y}{\partial y} = 0, \tag{27}$$

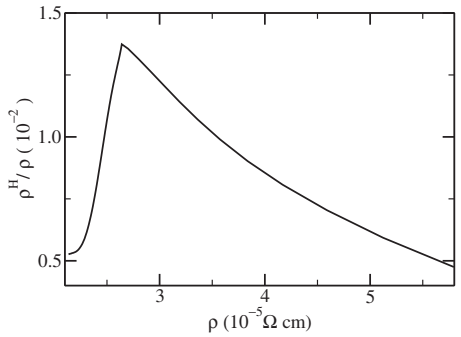

FIG. 6. Hall angle ρ^H/ρ as a function of $\rho=1/\sigma_{xx}$ with the same parameters as in Fig. 5.

$$\frac{\partial \vec{m}}{\partial t} + \frac{\partial j_m^x}{\partial x} + \frac{\partial j_m^y}{\partial y} = -\frac{\vec{m}}{\tau_{sf}}, \tag{28}$$

where n and $\vec{m}=\{0,0,m\}$ are charge and spin accumulations, respectively, $\vec{j_e}$ and $\vec{j_m}$ are charge and spin currents, respectively, and τ_{sf} is the spin-flip relaxation time.

For the stable state solution $\frac{\partial n}{\partial t}=\frac{\partial \vec{m}}{\partial t}=0$. For the charge and spin currents, we have the system of equations

$$j_e^x = \sigma_{xx}E - D_{xx}\left(\frac{\partial n}{\partial x} - \beta'\frac{\partial m}{\partial x}\right) - D_{xy}\left(\frac{\partial n}{\partial y} - \beta'\frac{\partial m}{\partial y}\right), \tag{29}$$

$$j_e^y = \sigma_{yx}E - D_{yy}\left(\frac{\partial n}{\partial y} - \beta'\frac{\partial m}{\partial y}\right) - D_{yx}\left(\frac{\partial n}{\partial x} - \beta'\frac{\partial m}{\partial x}\right), \tag{30}$$

$$j_m^x = \beta\sigma_{xx}E - D_{xx}\left(\beta'\frac{\partial n}{\partial x} - \frac{\partial m}{\partial x}\right) - D_{xy}\left(\beta'\frac{\partial n}{\partial y} - \frac{\partial m}{\partial y}\right), \tag{31}$$

$$j_m^y = \beta\sigma_{yx}E - D_{yy}\left(\beta'\frac{\partial n}{\partial y} - \frac{\partial m}{\partial y}\right) - D_{yx}\left(\beta'\frac{\partial n}{\partial x} - \frac{\partial m}{\partial x}\right), \tag{32}$$

where $\vec{E}=\{E,0,0\}$ is the electric field, $D_{\alpha\beta}$ and $\sigma_{\alpha\beta}$ denote the components of diffusion coefficient and conductivity tensor, respectively, β and β' are the coefficients of the spin asymmetry of these components. The off-diagonal components D_{xy} and σ_{xy} are proportional to the spin-orbit interaction and are antisymmetrical in the x-y transposition. For a metal with the cubic symmetry $\sigma_{xx}=\sigma_{yy}$ and $D_{xx}=D_{yy}\equiv D_0$.

We insert Eqs. (29)–(32) into Eqs. (27) and (28) and after some manipulations, we obtain two equations

$$\Delta n = -\beta'\Delta m, \tag{33}$$

$$\beta'\Delta n + \Delta m = \frac{m}{\tau_{sf}}. \tag{34}$$

Assuming that $\tau_{sf}D_0(1-\beta'^2)\equiv\lambda_{sf}^2$

$$\Delta m - \frac{m}{\lambda_{sf}^2} = 0. \tag{35}$$

For the cylindrical defect shape, it is convenient to search for solution in polar coordinates. For that, we rewrite Eq. (35) as

$$\frac{1}{r}\frac{\partial}{\partial r}\left(r\frac{\partial m}{\partial r}\right) + \frac{1}{r^2}\frac{\partial^2 m}{\partial \varphi^2} - \frac{m}{\lambda_{sf}^2} \equiv \frac{\partial^2 m}{\partial r^2} + \frac{1}{r}\frac{\partial m}{\partial r} + \frac{1}{r^2}\frac{\partial^2 m}{\partial \varphi^2} - \frac{m}{\lambda_{sf}^2} = 0, \tag{36}$$

where φ is the angle between x axis and the radius vector $\vec{r}$ with coordinates (x,y).

The solution of Eq. (36) is

$$m = m_1(r)m_2(\varphi), \tag{37}$$

$$m_2(\varphi) = A_{1n}\cos n\varphi + A_{2n}\sin n\varphi. \tag{38}$$

As $\frac{\partial^2 m_2}{\partial \varphi^2} = -m_2 n^2$, Eq. (36) can be transformed

$$m_2(\varphi)\left[\frac{\partial^2 m_1}{\partial r^2} + \frac{1}{r}\frac{\partial m_1}{\partial r} - \left(\frac{1}{\lambda_{sf}^2} + \frac{n^2}{r^2}\right)m_1\right] = 0. \tag{39}$$

The solution of Eq. (39) is

$$m_1(r) = B_k K_k\left(\frac{r}{\lambda_{sf}}\right), \tag{40}$$

$$m = \sum_n (A_{1n}\cos n\varphi + A_{2n}\sin n\varphi)K_k\left(\frac{r}{\lambda_{sf}}\right), \tag{41}$$

where $K_k(\frac{r}{\lambda_{sf}})$ is the solution of the modified Bessel equation.[16]

From Eq. (33), it follows that

$$n = -\beta' m + n_0, \tag{42}$$

$$\Delta n_0 = 0. \tag{43}$$

For n_0, the solution is

$$n_0 = \sum_n (C_{1n}\cos n\varphi + C_{2n}\sin n\varphi)\frac{1}{r^n}. \tag{44}$$

Taking into account Eq. (33), we can rewrite Eqs. (29) and (30)

$$j_e^x = \sigma_{xx}E - D_{xx}\frac{\partial n_0}{\partial x} - D_{xy}\frac{\partial n_0}{\partial y}, \tag{45}$$

$$j_e^y = \sigma_{yx}E - D_{yy}\frac{\partial n_0}{\partial y} + D_{yx}\frac{\partial n_0}{\partial x}. \tag{46}$$

It is now convenient to use the polar-coordinate system and to write down r and φ projections of the currents. Then we can use the boundary conditions to find the unknown coefficients. These projections are

$$j_{re}^0 = \sigma_{xx}E\cos\varphi + \sigma_{xy}E\sin\varphi \tag{47}$$

(usual term), and

$$\delta j_{re} = -D_{xx}\frac{\partial n_0}{\partial x}\cos\varphi - D_{xy}\frac{\partial n_0}{\partial y}\cos\varphi - D_{yy}\frac{\partial n_0}{\partial y}\sin\varphi + D_{xy}\frac{\partial n_0}{\partial x}\sin\varphi \tag{48}$$

(additional diffusion term).

We can now make some transformations

$$\frac{\partial n}{\partial x} = \frac{\partial n}{\partial r}\frac{\partial r}{\partial x} + \frac{\partial n}{\partial \varphi}\frac{\partial \varphi}{\partial x}, \tag{49}$$

$$\frac{\partial n}{\partial y} = \frac{\partial n}{\partial r}\frac{\partial r}{\partial y} + \frac{\partial n}{\partial \varphi}\frac{\partial \varphi}{\partial y}. \tag{50}$$

Using the expressions for derivatives of r and φ over x and y, which is not too difficult to obtain, we write down the charge and spin currents in polar coordinates as

$$\delta j_{re} = -D_0\frac{\partial n}{\partial r} - D_{xy}\frac{\partial n}{r\,\partial \varphi}, \tag{51}$$

$$\delta j_{rm}^n = -D_0\beta'\frac{\partial n}{\partial r} - D_{xy}\beta'\frac{\partial n}{r\,\partial \varphi}, \tag{52}$$

$$\delta j_{rm}^m = -D_0\frac{\partial m}{\partial r} - D_{xy}\frac{\partial m}{r\,\partial \varphi}, \tag{53}$$

$$\delta j_{rm}^0 = \beta\sigma_{xx}E\cos\varphi + \beta\sigma_{yx}E\sin\varphi. \tag{54}$$

To find the unknown coefficients in Eqs. (41) and (44), we use the boundary conditions on the surface of the cylinder, in other words, r projection of the currents at these boundaries are equal to zero,

$$j_R^{0n} + \delta j_R^n = 0 \Rightarrow D_0\left.\frac{\partial n_0}{\partial r}\right|_{r=R} + D_{xy}\left.\frac{\partial n_0}{R\,\partial \varphi}\right|_{r=R} = -D_0\sum_n (C_{1n}\cos n\varphi + C_{2n}\sin n\varphi)\frac{n}{R^{n+1}} - D_{xy}\sum_n (C_{1n}\sin n\varphi - C_{2n}\cos n\varphi)\frac{n}{R^{n+1}}. \tag{55}$$

This gives us the system

$$\sigma_{xx}E = -R^{-2}(D_0 C_{11} - D_{xy}C_{21}), \tag{56}$$

$$\sigma_{xy}E = R^{-2}(D_{xy}C_{11} + D_0 C_{21}), \tag{57}$$

with solution

$$C_{11} = -\frac{D_0\sigma_{xx} - D_{xy}\sigma_{xy}}{D_0^2 + D_{xy}^2}, \tag{58}$$

$$C_{21} = \frac{D_0\sigma_{xy} + D_{xy}\sigma_{xx}}{D_0^2 + D_{xy}^2}, \tag{59}$$

$$n_0 = -\frac{R^2 E}{r}\frac{1}{D_0^2 + D_{xy}^2}[(D_0\sigma_{xx} - D_{xy}\sigma_{xy})\cos\varphi - (D_0\sigma_{xy} + D_{xy}\sigma_{xx})\sin\varphi]. \quad (60)$$

The spin current r projection at the boundaries is also zero, which yields

$$j_R^{0m} + \delta j_R^m = 0 \Rightarrow \beta E(\sigma_{xx}\cos\varphi - \sigma_{xy}\sin\varphi) = D_0 \left.\frac{\partial m}{\partial r}\right|_{r=R} + D_{xy}\left.\frac{\partial m}{R\,\partial\varphi}\right|_{r=R} = D_0(A_{11}\cos\varphi + A_{21}\sin\varphi)\frac{\partial}{\partial r}K_1\left(\frac{r}{\lambda_{sf}}\right)\Bigg|_{r=R} + D_{xy}(-A_{11}\sin\varphi + A_{21}\cos\varphi)\frac{1}{R}K_1\left(\frac{R}{\lambda_{sf}}\right). \quad (61)$$

From Eq. (61) it follows that

$$A_{11} = \frac{\beta E(\sigma_{xx}D_0K_1'R + \sigma_{xy}D_{xy}K_1)R}{R^2(D_0K_1')^2 + (D_{xy}K_1)^2}, \quad (62)$$

$$A_{21} = -\frac{\beta E(-\sigma_{xx}D_{xy}K_1 + \sigma_{xy}D_0K_1'R)R}{R^2(D_0K_1')^2 + (D_{xy}K_1)^2}, \quad (63)$$

where $K_1' = \frac{\partial}{\partial r}K\left(\frac{r}{\lambda_{sf}}\right)|_{r\to R}$.

We can now define the additional Hall field due to these cylindrical topological defects, considering that the Hall electrodes are the surfaces with coordinates $y=a$ and $y=-a$. This field is proportional to $n(a)-n(-a)$, where $n=-\beta' m + n_0$. After averaging over the positions of the cylindrical defects, homogeneously distributed within the layer, the Hall drop of voltage reads

$$\Delta V_H^n = 2ER^2\frac{\sigma_{xy}}{\sigma_{xx}}\frac{a\pi}{\bar{R}^2}, \quad (64)$$

where $\bar{R}$ is the average distance between the defects.

For $R \ll \lambda_{sf} \ll a$, the second term $-\beta' m$ gives the contribution

$$\Delta V_H^m = -\beta\beta' ER\frac{\sigma_{xy}}{\sigma_{xx}}\frac{K_1 - RK_1'}{(RK_1')^2}\int_R^{2a-R} ydy \times \int_{-\infty}^{\infty}\frac{dx}{\sqrt{x^2+y^2}}K_1\left(\frac{\sqrt{x^2+y^2}}{\lambda_{sf}}\right) \approx -2\beta\beta'\frac{\sigma_{xy}}{\sigma_{xx}}\left(\frac{R}{\bar{R}}\right)^2\lambda_{sf}. \quad (65)$$

The ratio of $\Delta V_H = \Delta V_H^n + \Delta V_H^m$ to the original Hall voltage, $\Delta V_H^0 = 2Ea\frac{\sigma_{xy}}{\sigma_{xx}}$, for $R=1$ (nm) and $\bar{R}=10$ (nm), is estimated as

$$\frac{\Delta V_H^n + \Delta V_H^m}{\Delta V_H^0} \approx \frac{\Delta V_H^n}{\Delta V_H^0} = \frac{\pi R^2}{\bar{R}^2} \approx 0.03. \quad (66)$$

IV. CONCLUSION

It was shown that due to the additional scattering of electrons on the defects of the metal-insulator interfaces, the total conductance decreases. It follows from Eq. (22) that for small values of the ratio a/l, the bulk conductivity is completely suppressed and effective conductivity is proportional to the effective scattering length at the interfaces instead of the bulk mean-free path. If we do not take into account the additional skew scattering at the interfaces, the Hall conductivity decreases with decreasing the thickness of the ferromagnetic metallic layer. However, the contribution to the Hall conductivity due to the additional skew scattering at the interfaces increases. Therefore, the important characteristic of the considered device, Hall angle $\rho_{xy}/\rho_{xx} \approx \sigma_{xy}/\sigma_{xx}$, is larger for the thin ferromagnetic layer than for the bulk one. In addition, the presence of the insulator columns in the metallic layer may further increase the value of the Hall effect.

In order to experimentally observe these effects, one has to investigate the thickness dependence of the transport properties of a sandwich consisting of two insulating layers, for example, Al_2O_3 or MgO (interfaces F/amorphous Al_2O_3 usually contain more defects, which is favorable for the observation of the predicted effects), and a pure ferromagnetic layer with a large mean-free path (>100 Å), such as Ni, Co, or Fe. However, when comparing the experimental results with our predictions (see Fig. 6), one has to treat with caution the region of high resistivity, where possible influence of the side-jump scattering may give additional contribution to ρ dependence of EHE.

ACKNOWLEDGMENTS

N. Ryzhanova and A. Vedyayev are grateful to SPINTEC for hospitality. This work was partially supported by the Russian Foundation for Basic Research.

APPENDIX

In this additional section we present the details of the calculation of the conductivity tensor. The complete expression for the bulk quasi-two-dimensional diagonal conductivity is

$$\sigma_{xx}^{\uparrow} = \frac{\sigma_0 l_1 10^8}{2\pi k_F^{\uparrow}}\int\frac{\kappa^3 d\kappa Nom_1^{\uparrow}}{c_1 Den_1^{\uparrow}}, \quad (A1)$$

where

$$Nom_1^{\uparrow} = (q^2 + c_1^2)[2c_1|\mathrm{Im}\,\Sigma|\cosh 2d_1 a + (q^2 + c_1^2 + |\Sigma|^2 + 2q\,\mathrm{Re}\,\Sigma)\sinh 2d_1 a] - 2c_1(q + \mathrm{Re}\,\Sigma)(q^2 + c_1^2)\sinh 2d_1(z-a)\sin 2c_1 z + 2c_1\,\mathrm{Im}\,\Sigma^{-}\{2\sinh^2 d_1 z[\cos 2c_1(z-a) + 2qc_1\sin 2c_1(z-a)] + (q^2 + c_1^2)\cosh 2d_1(z-a)\} + (q^2 + c_1^2 + |\Sigma|^2 + 2q\,\mathrm{Re}\,\Sigma)\{(q^2 + c_1^2)\sinh 2d_1(z-a)\cos 2c_1 z - \sinh 2d_1 z[(q^2 - c_1^2)\cos 2c_1(z-a) + 2qc_1\sin 2c_1(z-a)]\}, \quad (A2)$$

$$Den_1^{\uparrow} = (q^2 + c_1^2)[2c_1|\mathrm{Im}\,\Sigma|\sinh 2d_1 a + (q^2 + c_1^2 + |\Sigma|^2 + 2q\,\mathrm{Re}\,\Sigma)\cosh 2d_1 a] - [q^4 - 6q^2c_1^2 + c_1^4 + (|\Sigma|^2 + 2q\,\mathrm{Re}\,\Sigma)(q^2 - c_1^2) - 4qc_1^2\,\mathrm{Re}\,\Sigma]\cos 2c_1 a - 2qc_1[2(q^2 - c_1^2 + q\,\mathrm{Re}\,\Sigma) + |\Sigma|^2]\sin 2c_1 a. \quad \text{(A3)}$$

Equation (22) was obtained from the above formula by averaging out the oscillatory terms. The off-diagonal conductivity due to the spin-orbit interfacial scattering is calculated using Eqs. (10) and (21) with $z''=0$ by integrating over z'

$$\sigma_{xy}^{\uparrow} = \frac{\sigma_0 l_1 a_0^4 10^8}{2\pi^2 k_F^{\uparrow}} \int \frac{\kappa^3 d\kappa c_1}{Den_2^{\uparrow}} \mathrm{Im}\langle T(\vec{\rho}_n 0)\lambda^{so}(\vec{\rho}_n 0)\rangle (q^2 + c_1^2)\sinh 2d_1 a \times \int \frac{\kappa^3 d\kappa}{Den_2^{\uparrow}}[(q^2 + c_1^2)\cosh 2d_1(z-a) - (q^2 - c_1^2)\cos 2c_1(z-a) - 2c_1 q\,\sin 2c_1(z-a)], \quad \text{(A4)}$$

where

$$Den_2^{\uparrow} = \left| e^{ik_1 a}(q + ic_1)^2\left(1 + \frac{\Sigma^-}{q + ic_1}\right) - e^{-ik_1 a}(q - ic_1)^2\left(1 + \frac{\Sigma^-}{q - ic_1}\right)\right|^2. \quad \text{(A5)}$$

One can see from Eq. (A5) that $\sigma_{xy}^{\uparrow}$ oscillates with the thickness a and the distance from the interface $z=0$. Its behavior becomes more clear after averaging over oscillations that was done in Eq. (23).

As it was already mentioned in Sec. II B, the bulk off-diagonal conductivity σ_{xy}^{bulk} is calculated using Eq. (10) with the bulk scattering parameters and the bulk coherent potential in Born approximation. In the absence of the interfacial scattering, this approach yields

$$\sigma_{xy}^{\uparrow bulk} = \frac{\sigma_0 l_1^2 a_0^3\,\mathrm{Im}\langle T^{bulk}\lambda_{bulk}^{so}\rangle 10^8}{8\pi^2 k_F^{\uparrow 2}} \times \int \frac{\kappa^3 d\kappa}{c_1}\frac{(q^2 + c_1^2)^2 \sinh 2d_1 a}{Den_4^{\uparrow}} \times \int \frac{\kappa^3 d\kappa}{c_1}\frac{1}{Den_4^{\uparrow}} \times \{(q^2 + c_1^2)^2 \sinh 2d_1 a - (q^4 - c_1^4)[\sinh 2d_1 z\,\cos 2c_1(z-a) - \sinh 2d_1(z-a)\cos 2c_1 z] + 2qc_1[\sinh 2d_1 z\,\sin 2c_1(z-a) + \sinh 2d_1(z-a)\sin 2c_1 z]\}, \quad \text{(A6)}$$

where

$$Den_4^{\uparrow} = \cosh 2d_1 a(q^2 + c_1^2)^2 - (q^4 - 6q^2c_1^2 + c_1^4)\cos 2c_1 a + 4c_1 q(q^2 - c_1^2)\sin 2c_1 a. \quad \text{(A7)}$$

[1] J. S. Moodera, L. R. Kinder, T. M. Wong, and R. Meservey, Phys. Rev. Lett. **74**, 3273 (1995).
[2] J. C. Slonczewski, J. Magn. Magn. Mater. **159**, L1 (1996).
[3] J. Smit, Physica **24**, 39 (1958).
[4] J. M. Luttinger, Phys. Rev. **112**, 739 (1958).
[5] L. Berger, Phys. Rev. B **2**, 4559 (1970); **5**, 1862 (1972).
[6] A. Crepieux and P. Bruno, Phys. Rev. B **64**, 014416 (2001).
[7] R. Karplus and J. M. Luttinger, Phys. Rev. **95**, 1154 (1954).
[8] M. Onoda and N. Nagaosa, Phys. Rev. Lett. **90**, 206601 (2003); Z. Fang, Naoto Nagaosa, Kei S. Takahashi, Atsushi Asamitsu, Roland Mathieu, Takeshi Ogasawara, Hiroyuki Yamada, Masashi Kawasaki, Yoshinori Tokura, and Kiyoyuki Terakura, Science **302**, 92 (2003).
[9] T. Jungwirth, Q. Niu, and A. H. MacDonald, Phys. Rev. Lett. **88**, 207208 (2002); D. Culcer, J. Sinova, N. A. Sinitsyn, T. Jungwirth, A. H. MacDonald, and Q. Niu, *ibid.* **93**, 046602 (2004); V. K. Dugaev, P. Bruno, M. Taillefumier, B. Canals, and C. Lacroix, Phys. Rev. B **71**, 224423 (2005).
[10] T. S. Nunner, N. A. Sinitsyn, Mario F. Borunda, V. K. Dugaev, A. A. Kovalev, Ar. Abanov, Carsten Timm, T. Jungwirth, Junichiro Inoue, A. H. MacDonald, and Jairo Sinova, Phys. Rev. B **76**, 235312 (2007).
[11] N. A. Sinitsyn, A. H. MacDonald, T. Jungwirth, V. K. Dugaev, and J. Sinova, Phys. Rev. B **75**, 045315 (2007).
[12] A. A. Kovalev, K. Vyborny, and J. Sinova, Phys. Rev. B **78**, 041305(R) (2008).
[13] S. Onoda, N. Sugimoto, and N. Nagaosa, Phys. Rev. B **77**, 165103 (2008).
[14] N. Ryzhanova, A. Vedyayev, A. Crepieux, and C. Lacroix, Phys. Rev. B **57**, 2943 (1998).
[15] S. Zhang, P. M. Levy, and A. Fert, Phys. Rev. Lett. **88**, 236601 (2002).
[16] A. N. Tikhonov and A. A. Samarskii, *Equations of Mathematical Physics* (Pergamon Press, Oxford, London, 1963), p. 656.